Investigation of the longitudinal magnetic field effect in $SmBa_2Cu_3O_y$ films with various shaped artificial pinning centers

K Sugihara[1], Y Ichino[1], Y Tsuchiya[1], A Ichinose[2] and Y Yoshida[1]

[1] Department of Energy Engineering and Science, Nagoya University, Furo-cho, Chikusa Nagoya 464-8603, Japan

[2] Central Research Institute of Electric Power Industry, 2-6-1 Nagasaka, Yokosuka, Kanagawa 240-0196, Japan

E-mail: sugihara-kazuki14@ees.nagoya-u.ac.jp

Abstract

The longitudinal magnetic field (LMF) state, in which the magnetic field is applied parallel to the applied current direction and *ab*-plane of $SmBa_2Cu_3O_y$ (Sm123) films with shaped artificial pinning centers (APCs) of various shapes is investigated. The in-field critical current density (J_c) of pure Sm123 films in the LMF state and films with Y_2O_3, Sm_2BaCuO_5, $BaHfO_3$, and multilayered-structure with short $BaHfO_3$ nanorods were measured in the configuration. The measurement revealed that there was significant J_c enhancement only in the multilayered-film. From the viewpoint of flux pinning, 3D-flux pinning is the key to improving in-field J_c in the LMF state. However, the Sm123 films with APCs, such as Y_2O_3 and Sm_2BaCuO_5, did not have a larger J_c than the pure Sm123 films in the LMF state. This indicates that the APCs prevent the current flowing along the external magnetic field. Both of the 3D-flux pinning and the pure layer in which current can flow without disturbance are important for the J_c enhancement in the LMF state.

Keywords: Cuprates, Critical current, Flux pinning, Thin films, Multilayers

1. Introduction

Recently, many manufactures have developed high temperature superconducting (HTS) wires, such as $Bi_2Sr_2Ca_2Cu_3O_y$ (Bi-2223) and $REBa_2Cu_3O_y$ (RE123, RE = rare earth), for the next generation of superconducting applications. The HTS wires carry supercurrents even at liquid N_2 temperature; therefore, the cost for the refrigerant can be saved [1-3]. In fact, Bi-2223 and $YBa_2Cu_3O_y$ (Y123) cables already have been introduced into DC power transmission [4]. Additionally, the RE123-coated conductors have great potential for high-field superconducting magnets [1-3]; therefore, there have been many studies to improve the in-field properties of RE123 by adding artificial pinning centers (APCs) into the RE123 matrix [7-37]. The well-investigated APC materials for the improvement of the properties are nonsuperconductors, such as metallic nanodots of Ag [8-10, 13, 20, 21], Au [10, 13, 20], substrate decoration [8-13, 20, 21], quasimultilayer technique [12, 13, 20, 21], heavy-ion irradiation [14], $BaMO_3$ (BMO, M = metal: Zr, Sn, Hf) [15-26], $Ba_2RE(Nb, Ta)O_6$ [27-31], RE_2O_3 [25, 32, 33], RE_2BaCuO_5 (RE211) [34-36], and $Gd_2Ba_4CuWO_y$ [37].

However, the reduction of the Lorentz force (F_L) on flux lines is also effective to improve the critical current density (J_c). The F_L on the flux lines is formulated as the cross product between vectors of current and flux density; therefore, it disappears when these vectors are parallel namely, in a longitudinal magnetic field (LMF) state. Additionally, LMF effects comprising various peculiar electromagnetic phenomena have been reported [38]. In general, in transverse magnetic fields, J_c monotonically decreases with increasing the fields. However, J_c enhancement by the LMF effect in a certain magnetic field compared with that in a self-field has been reported, and it is called "J_c-gain" [39-42]. The J_c-gain has great potential to increase the current capacity of superconducting power cables. For saving space and cost, Matsushita *et al*. suggested a novel architecture of superconducting power cables with high efficiency [43-46]. This cable applies the LMF state via the peculiar design of tape winding in which the synthetic vector field consisting of the external field and its self-field becomes parallel to the current. Recently, current capacity enhancement in Bi-2223 tapes was reported with a cable architecture, as suggested previously [46].

The J_c-gain in the LMF state in $SmBa_2Cu_3O_y$ (Sm123) films with multilayered (ML)-architecture [47-50] consisting of pure Sm123 and $BaHfO_3$ (BHO)-doped Sm123 layers has been reported. The J_c-gain at liquid N_2 temperature was observed not in pure Sm123 films, but in the ML-Sm123 films. However, some researchers have reported the J_c-gain in pure Y123 films with a single-layer structure [41].

The ML-structure could be suitable for J_c-gain appearance; however, its mechanism is still

unclear in terms of flux pinning, APC shape, and film structure. Flux motion is in a spiral shape in the LMF state, and it is necessary to consider the flux pinning effect with separated directions on the complicated flux motion. In this study, the focus is on the relationship between the F_L directions, such as in-plane and out-of-plane, and the J_c property in the LMF state in several Sm123 films with various APCs. From this investigation, it is possible to clarify the dominant factor for the J_c gain in terms of flux pinning. Therefore, a study was conducted upon the in-field properties in the transverse field and the LMF state in a pure Sm123 film and Sm123 films with randomly distributed nanoparticles such as Y_2O_3 and Sm_2BaCuO_5 (Sm211), BHO nanorods threading a film, and ML-structure.

2. Experimental procedure

Pure and APC-doped Sm123 films on $LaAlO_3$ (100) single-crystalline substrates were fabricated by the pulsed laser deposition method using a KrF excimer laser (λ = 248 nm) at a repetition rate of 10 Hz. Y_2O_3, Sm211, and BHO were chosen as APCs in this study, because they have been reported to form nanoparticles or nanorods in the RE123 matrix [22-26,32-36]. To dope the APCs into the Sm123 matrix, a surface modified target technique was used in which a Sm123-sintered bulk as a target was modified by putting thin sectors of Y_2O_3 or Sm211 onto the Sm123 target by means of a silver paste. A 3 vol% BHO mixed Sm123 target was used to deposit a Sm123 film with BHO nanorods. Additionally, an ML film were deposited with pure and 3 vol% BHO mixed Sm123 targets by an alternating target technique [23], and this film had 48 layers (48ML), which were alternately stacked 24 pure and 24 BHO-doped layers each of a thickness of around 8 nm. BHO nanorods in the 48ML film were cut to short lengths by the pure layers. The distance between the targets and the substrate was 50 mm. The substrate temperature was kept at 860 ºC. The O_2 partial pressure was 53 Pa during the deposition. The laser energy density was 1.6 J/cm^2. Additionally, these films had a total film thickness of approximately 400 nm. X-ray diffraction analysis was used to evaluate the film crystallinity. The film thickness was measured by an optical interferometry microscope. The films were patterned into bridge shapes, with a width of 0.1 mm and a length of around 1 mm, using laser etching. Superconducting properties were measured using the standard four-probe method in external magnetic fields with various directions. The J_c were evaluated from *I-V* curves with an electric field criterion of 1.0 μV/cm.

3. Results and discussion

First, the crystallinity of the Sm123 films was evaluated. All the films had epitaxial growth on the substrates and had a negligible amount of *a*-axis-oriented phase. The critical temperatures (T_cs) and J_cs in the self-field (J_c^{self}s) at 77 K are listed in Table 1.

The film structures of these samples were evaluated in terms of in-field properties. Figure 1 shows the angular dependence of the transverse in-field J_c at 77 K in 1 T. Figure 1 shows that the Y_2O_3 samples had particle-like pinning centers, because they show a similar J_c property to one found in a previous report [33]. Y_2O_3 had a shape in nanoparticle with a diameter of 10-20 nm and the random configuration in the Sm123 matrix from a previous report [25], because the conditions in the film deposition were almost the same. Although the Sm211 sample showed isotropic in-field J_c, lower J_c and lower T_c values were observed. It is thought that Sm211 also shaped random nanoparticles and their diameters were more than 10 nm from a similar report of Y_2BaCuO_5 [36]. In addition, RE123 of light rare earths (LREs), such as La, Nd, and Sm, form a solid solution $LRE_{1+x}Ba_{2-x}Cu_3O_y$ via an RE/Ba solid solution [51, 52]. In Sm123, the Sm/Ba solid solution spread with the size of more than 100 nm in the Sm123 matrix, and the T_c decreased with increasing Sm/Ba solid solution [52]. In this study, the Sm211 sample had not only Sm211 particles, but also Sm/Ba solid solution, because the Sm211 sample showed lower T_c than the pure sample. The above demonstrates that the Sm211 and Sm/Ba solid solution within the Sm123 matrix could have a larger diameter or higher number density of particles. The 48ML sample showed isotropic enhancement compared with the pure sample, and, especially, it showed higher J_c around $B \parallel ab$ than that of the other samples by strong pinning via a stacking interface parallel to the *ab*-plane. From this result and a previous report [23], it can be concluded that the 48ML sample has an ML-structure. The BHO sample showed a sharp J_c peak around $B \parallel c$; thus, BHO becomes nanorods threading the Sm123 film [24]. From previous research [49], BHO nanorods diameters were approximately 10 nm in the 48ML and the BHO samples, because the film deposition conditions were almost the same.

Figure 2(a) shows the J_c-B curves in the LMF state at 77 K. Figure 2(b) shows the ones normalized by each J_c^{self} and the magnified plot in the low-field region. As a notable result, a J_c-gain was observed only in the 48ML sample. The J_c-gain was defined as a J_c enhancement in a certain magnetic field in comparison with the J_c^{self}. In the normalized data, the pure sample showed comparatively higher J_c than the other samples with APCs, except for the 48ML sample. Other notable data were samples with "random" nanoparticles such as Y_2O_3 or Sm211. The Y_2O_3 sample showed a higher J_c around $B \parallel ab$ than the pure sample in Figure 1; however, the in-field J_c in the LMF state was almost equal to that of the pure sample in Figure 2. Also, the Sm211

sample showed a similar tendency to that of the Y_2O_3 sample. The BHO sample showed the lowest property among the samples.

For the LMF state, one should consider the flux pinning with respect to the spiral motion of flux lines [38]. The spiral motion can be simplified as in-plane and out-of-plane directions for the films. There should be suitable shapes of pinning centers for the several directions of the flux lines; then, the flux pinning force (F_p) property was examined. The above-mentioned were considered with separated F_L along the *c*-axis direction and F_L parallel to the *ab*-plane. The relationship between F_p for both the directions and the J_c in the LMF state at 1 T in 77 K is represented in Figure 3. This figure shows the separated flux pinning effect on the J_c in the LMF state. From this figure, one can see that there is a roughly linear relationship between the F_p in $F_L \parallel c$ and the J_c in the LMF state, except for the Y_2O_3 sample. We discuss this tendency of Y_2O_3 later. However, there is no definite tendency for the F_p in $F_L \parallel ab$. The 48ML sample was the highest F_p and J_c among the samples. The Y_2O_3 sample showed higher F_p than the pure sample both of $F_L \parallel ab$ and $F_L \parallel c$, and the BHO sample showed higher F_p in $F_L \parallel ab$ than the pure sample. However, the Y_2O_3 and the BHO samples showed a lower J_c in the LMF state than the pure sample. The Sm211 sample showed lower F_p and J_c in the LMF state. It is considered that too large or high a number density of particles did not pin flux effectively in a transverse and a longitudinal magnetic field.

It was expected that the 3D-flux pinning would be effective for the J_c enhancement in the LMF state, because flux lines move in a spiral shape along the current direction. From a previous report [48] and the results from Figures 1 through 3, flux pinning along the *c*-axis direction had a larger influence on the in-field property in the LMF state than that along the *ab*-plane. There was a roughly linear relationship between F_p in $F_L \parallel c$ and J_c in the LMF state, as shown in Figure 3, and the higher F_p in $F_L \parallel c$ sample shows a comparatively higher J_c in the LMF state.

These results illustrate the flux motion in a superconducting film in the LMF state and its pinning around the film surface, as shown in Figure 4. Flux lines penetrate toward the center of the film from the surface, and the flux lines instantaneously release the rotational strain (force-free torque) caused by the self-field. Then, a critical state is determined by the equilibrium of the force-free torque and its pinning (pinning torque). The J_c in this state becomes higher with increasing pinning centers that can pin the rotation of flux lines. There is a report that described a linear relationship between the J_c in the LMF state and the pinning torque [53]. Flux lines at the sides of the film move to the center of the film along a direction of the *ab*-plane. In general, the self-field is maximum at an edge of a film with the direction along the *c*-axis, so that the pinning torque at the edge has more influence on the critical state than that at the top surface of the film. Therefore, the flux pinning along the *c*-axis direction at the edge mainly determines the whole critical state, because the flux pinning along the *c*-axis can suppress the distortion of the flux lines

at the edge. In other words, flux pinning for $F_L//c$ is effective for an enhancement of J_c in the LMF state; therefore, pinning centers such as the interface of pure and BHO-doped layers are useful. This speculation is also supported from a previous report [48] and the results of Figures 1 through 3 that the sample with 3D-pinning centers, such as the Y_2O_3 and the 48ML samples, showed a higher J_c in the LMF state than the BHO sample with a 1D-pinning center.

The above shows that the Y_2O_3 sample with a higher F_p than the pure sample should have a higher J_c in the LMF state than that of the pure sample. For consideration of the differences among the pure, Y_2O_3, and 48ML samples, the APCs configuration was examined. First, the pure sample had no APCs. The Y_2O_3 sample had randomly distributed nanoparticles, and the 48ML sample had short BHO nanorods separated by pure layers. In other words, there were pure layers with no APCs in the pure and 48ML samples. In the LMF state, the critical current became higher when the current and magnetic field were parallel, because the F_L became zero theoretically. It is considered that the current can flow without disturbance in the pure layer, and 3D-APCs can trap the flux lines in the LMF state. Therefore, the Y_2O_3 sample did not show the J_c gain in Figure 2 and showed a higher F_p and not-so-high J_c in the LMF state in Figure 3. Thus, the 48ML sample, which had both a pure layer and the 3D-APCs, showed the highest J_c in the LMF state.

4. Conclusions

The LMF effect in the pure Sm123 films and those with several shaped APCs, such as randomly distributed nanoparticles made of Y_2O_3 or Sm211, BHO nanorods, and ML-Sm123, was studied to investigate the flux pinning and the other factors for larger J_c enhancement. First, the angular dependence of in-field J_c of several samples was examined, and these films had the expected film structures. In the LMF state, J_c-gain was observed only in the 48ML sample. The Y_2O_3 sample showed a higher F_p in both $F_L \parallel ab$ and $F_L \parallel c$; however, the in-field J_c in the LMF state was lower than that of the pure sample. The Sm211 sample showed a lower F_p in the transverse field and J_c in the LMF state, because too large or high a number density of Sm211 or Sm/Ba solid solution did not pin flux effectively. In terms of the flux pinning, it is considered that the 3D-APCs are effective for the flux motion in the LMF state, because flux lines move in a spiral shape. Thus, it is important to enhance the supercurrent in the LMF state so that the current and field are parallel to each other. It is speculated that the current flow without a disturbance in the superconducting matrix is another factor for higher J_c in the LMF state. The ML-structure can pin flux lines that move in a spiral shape, and the current can flow without disturbance in the pure layers. Therefore, both the 3D-flux pinning and the pure layer in which current can flow without disturbance are effective for the J_c-gain and its enhancement.

Acknowledgment

This work was supported in part by the JSPS KAKENHI (16K20898 and 17J11158) and JST-ALCA. We thank Dr. T. Izumi, Dr. A. Ibi and Dr. T. Machi for assistance with IBAD-MgO buffered metal tapes.

References

[1] Larbalestier D, Gurevich A, Feldmann D M and Polyanskii A 2001 *Nature* **414** 368

[2] Shiohara Y, Taneda T and Yoshizumi M 2012 *Jpn. J. Appl. Phys.* **51** 010007

[3] Obradors X and Puig T 2014 *Supercond. Sci. Technol.* **27** 044003

[4] Maruyama O, Honjo S, Nakano T, Masuda T, Watanabe M, Ohya M, Yaguchi H, Nakamura N and Machida A 2014 *IEEE Trans. Appl. Supercond.* **25** 5401606

[5] Weber C S, Reis C T, Dada A, Masuda T and Moscovic J 2005 *IEEE Trans. Appl. Supercond.* **15** 1793

[6] Yumura H, Ashibe Y, Itoh H, Ohya M, Watanabe M, Masuda T and Weber C S 2009 *IEEE Trans. Appl. Supercond.* **19** 1698

[7] Matsushita T 2000 *Supercond. Sci. Technol.* **13** 730

[8] Ionescu M, Li A H, Zhao Y, Liu H K and Crisan A 2004 *J. Phys. D: Appl. Phys.* **37** 1824

[9] Mikheenko P, Tanner J L, Bowen J, Sarkar A, Dang V S, Abell J S and Crisan A 2010 *Physica C* **470** S234

[10] Mikheenko P, Sarkar A, Dang V S, Tanner J L, Abell J S and Crisan A 2009 *Physica C* **469** 798

[11] Matsumoto K, Horide T, Osamura K, Mukaida M, Yoshida Y, Ishinose A and Horii S 2004 *Physica C* **412-414** 1267

[12] Sarkar A, Mikheenko P, Dang V S, Abell J S and Crisan A 2009 *Physica C* **469** 1550

[13] Mikheenko P, Sarkar A, Dang V S,Tanner J L, Awang Kechik M M, Abell J S and Crisan A 2009 *IEEE Trans. Appl. Supercond.* **19** 3491

[14] Sueyoshi T, Ishikawa N, Iwase A, Chimi Y, Kiss T, Fujiyoshi T and Miyahara K 1998 *Physica C* **309** 79

[15] Macmanus-Driscoll J L, Foltyn S R, Jia Q X, Wang H, Serquis A, Civale L, Maiorov B, Hawley M E, Maley M P and Peterson D E 2004 *Nat. Mater.* **3** 439

[16] Yamada Y, Takahashi K, Kobayashi H, Konishi M, Watanabe T, Ibi A, Muroga T, Miyata S, Kato T, Hirayama T and Shiohara Y 2005 *Appl. Phys. Lett.* **87** 132502

[17] Varanasi C V, Burke J, Brunke L, Wang H, Sumption M and Barnes P N 2007 *J. Appl. Phys.* **102** 063909

[18] Mele P, Matsumoto K, Horide T, Ichinose A, Mukaida M, Yoshida Y, Horii S and Kita R 2008 *Supercond. Sci. Technol.* **21** 032002

[19] Crisan A, Awang Kechik M M, Mikheenko P, Dang V S, Sarkar A, Abell J S, Paturi P and Huhtinen H 2009 *Supercond. Sci. Technol.* **22** 045014

[20] Mikheenko P, Dang V S, Tse Y Y, Awang Kechik M M, Paturi P, Huhtinen H, Wang Y Sarkar A, Abell J S and Crisan A 2010 *Supercond. Sci. Technol.* **23** 125007

[21] Mikheenko P, Dang V S, Awang Kechik M M, Sarkar A, Paturi P, Huhtinen H, Abell J S and Crisan A 2011 *IEEE Trans. Appl. Supercond.* **21** 3184

[22] Tobita H, Notoh K, Higashikawa K, Inoue M, Kiss T, Kato T, Hirayama T, Yoshizumi M, Izumi T and Shiohara Y 2012 *Supercond. Sci. Technol.* **25** 062002

[23] Tsuruta A, Yoshida Y, Ichino Y, Ichinose A, Matsumoto K and Awaji S 2013 *Jpn. J. Appl. Phys.* **52** 010201

[24] Tsuruta A, Yoshida Y, Ichino Y, Ichinose A, Matsumoto K and Awaji S 2014 *Supercond. Sci. Technol.* **27** 065001

[25] Watanabe Y, Ichino Y, Yoshida Y and Ichinose A 2016 *Jpn. J. Appl. Supercond.* **55** 073101

[26] Tsuchiya Y, Miura S, Awaji S, Ichino Y, Matsumoto K, Izumi T, Watanabe K and Yoshida Y 2017 *Supercond. Sci. Technol.* **30** 104004

[27] Kai H, Mukaida M, Teranishi R, Mori N, Yamada K, Horii S, Ichinose A, Kita R, Matsumoto K, Yoshida Y, Awaji S, Watanabe K, Namba M and Fujiyoshi T 2008 *Physica C* **468** 1854

[28] Ercolano G, Bianchetti M, Wimbush S C, Harrington S A, Wang H, Lee J H and MacManus-Driscoll J L 2011 *Supercond. Sci. Technol.* **24** 095012

[29] Opherden L, Sieger M, Pahlke P, Hühne R, Schultz L, Meledin A, Tandeloo G, Nast R, Holzapfel B, Bianchetti M, MacManus-Driscoll J L and Hänisch J 2016 *Sci. Rep.* **6** 21188

[30] Ichino Y, Kusafuka Y, Ichinose A and Yoshida Y 2017 *Jpn. J. Appl. Phys.* **56** 073101

[31] Kusafuka Y, Ichino Y, Tsuchiya Y, Ichinose A and Yoshida Y 2017 *Supercond. Sci. Technol.* **30** 125008

[32] Gapud A A, Kumar D, Viswanathan S K, Cantoni C, Varela M, Abiade J, Pennycook S J and Christen D K 2005 *Supercond. Sci. Technol.* **18** 1502

[33] Mele P, Matsumoto K, Horide T, Ichinose A, Mukaida M, Yoshida Y and Horii S 2007 *Supercond. Sci. Technol.* **20** 616

[34] Haugan T, Barnes P N, Maartense I and Cobb C B 2003 *J. Mater. Res.* **18** 2618

[35] Haugan T, Barnes P N, Wheeler R, Meisenkothen F and Sumption M 2004 *Nature* **430** 867

[36] Jha A K, Matsumoto K, Horide T, Saini S, Mele P, Ichinose A, Yoshida Y and Awaji S 2017 *J. Appl. Phys.* **122** 093905

[37] Awang Kechik M M, Mikheenko P, Sarkar A, Dang V S, Hari Babu N, Cardwell D A, Abell J S and Crisan A 2009 *Supercond. Sci. Technol.* **22** 034020

[38] Matsushita T 2012 *Jpn. J. Appl. Phys.* **51** 010111

[39] Bychkov Yu F, Vereshchagin V G, Zuev M T, Karasik V R, Kurganov G B and Mal'tsev V A 1969 *JETP Lett.* **9** 404

[40] Cullen G W, Cody G D and McEvoy Jr. J P 1963 *Phys. Rev.* **132** 577

[41] Maiorov B, Jia Q X, Zhou H, Wang H, Li Y, Kursunovic A, MacManus-Driscoll J L, Haugan T J, Barnes P N, Foltyn S R and Civale L 2007 *IEEE Trans. Appl. Supercond.* **17** 3697

[42] Kido R, Kiuchi M, Otabe E S, Matsushita T, Jha A K, Matsumoto K 2016 *Phys. Procedia* **81** 117

[43] Matsushita T, Kiuchi M and Otabe E S 2012 *Supercond. Sci. Technol.* **25** 125009

[44] Matsushita T, Vyatkin V S, Kiuchi M and Otabe E S 2014 *AIP Conf. Proc.* **1574** 225

[45] Vyatkin V S, Kiuchi M, Otabe E S, Ohya M and Matsushita T 2015 *IEEE Trans. Appl. Supercond.* **25** 5400404

[46] Vyatkin V S, Kiuchi M, Otabe E S, Ohya M and Matsushita T 2015 *Supercond. Sci. Technol.* **28** 015011

[47] Tsuruta A, Watanabe S, Ichino Y and Yoshida Y 2014 *Jpn. J. Appl. Phys.* **53** 078003

[48] Sugihara K, Ichino Y and Yoshida Y 2015 *Supercond. Sci. Technol.* **28** 101004

[49] Sugihara K, Shimazaki N, Ichino Y and Yoshida Y 2016 *IEEE Trans. Appl. Supercond.* **26** 8001704

[50] Sugihara K, Ichino Y, Yoshida Y and Ichinose A 2016 *J. Japan Inst. Met. Mater.* **80** 439

[51] Murakami M, Sakai N, Higuchi T and Yoo S I 1996 *Supercond. Sci. Technol.* **9** 1015

[52] Miura M, Itoh M, Ishino Y, Yoshida Y, Takai Y, Matsumoto K, Ichinose A, Horii S and Mukaida M 2005 *IEEE Trans. Appl. Supercond.* **15** 3078

[53] Matsushita T, Miyamoto Y, Kikitsu A and Yamafuji K 1986 *Jpn. J. Appl. Phys.* **25** L725

Table 1

T_c and J_c^{self}s at 77 K of Sm123 films.

APC (architecture)	Sample name	T_c (K)	J_c^{self} at 77 K (MA/cm^2)
Pure	Pure	91.5	2.2
5 area% Y_2O_3 (random particles)	Y_2O_3	88.5	1.5
5 area% Sm211 (random particles)	Sm211	88.7	1.0
3 vol% BHO (threading nanorods)	BHO	90.8	1.7
48ML (multilayer)	48ML	91.7	2.7

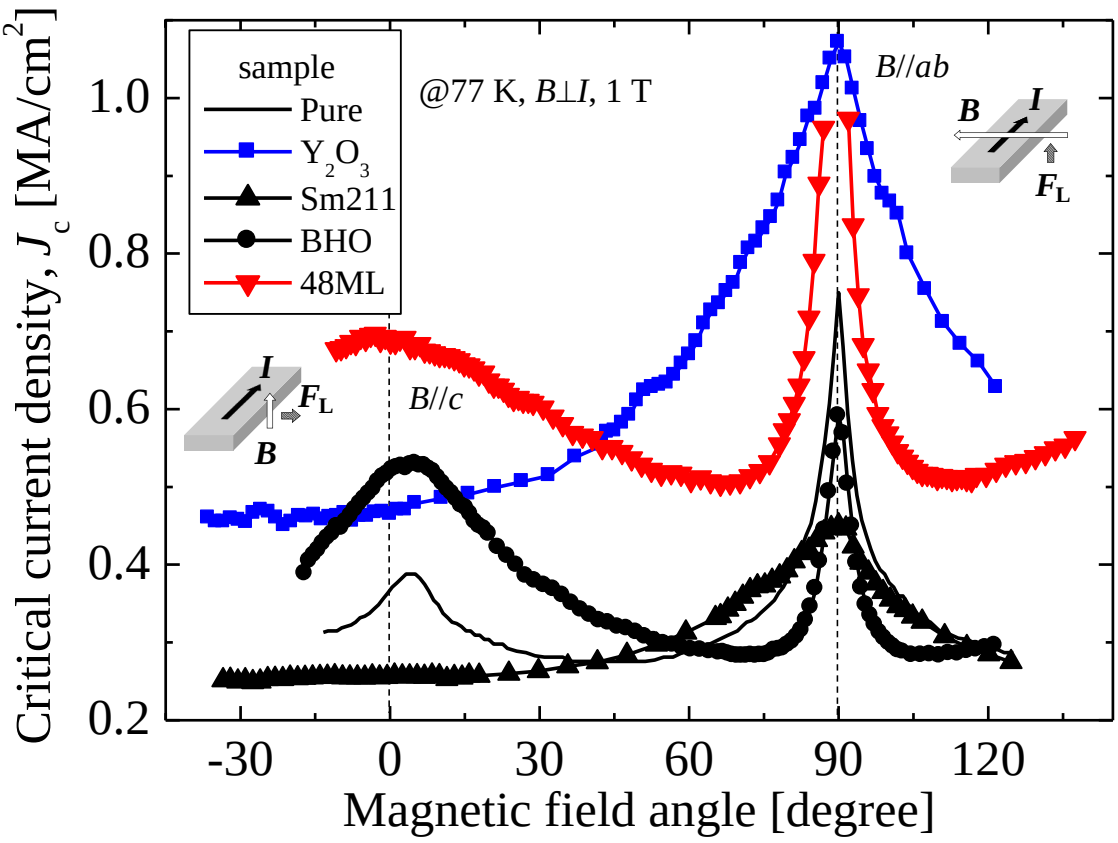

Figure 1

Angular dependence of in-field J_c at 77 K in 1 T of each Sm123 film.

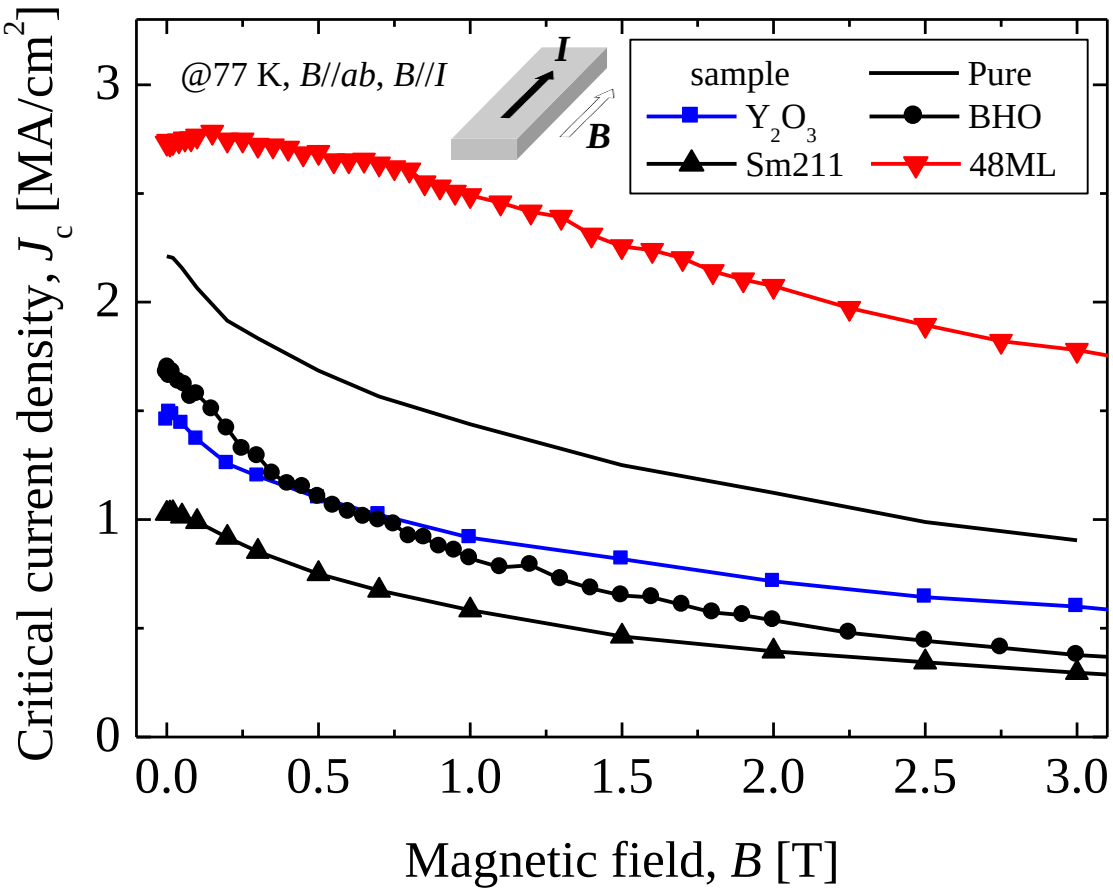

Figure 2(a)

J_c-B curves of each Sm123 film at 77 K in the LMF state.

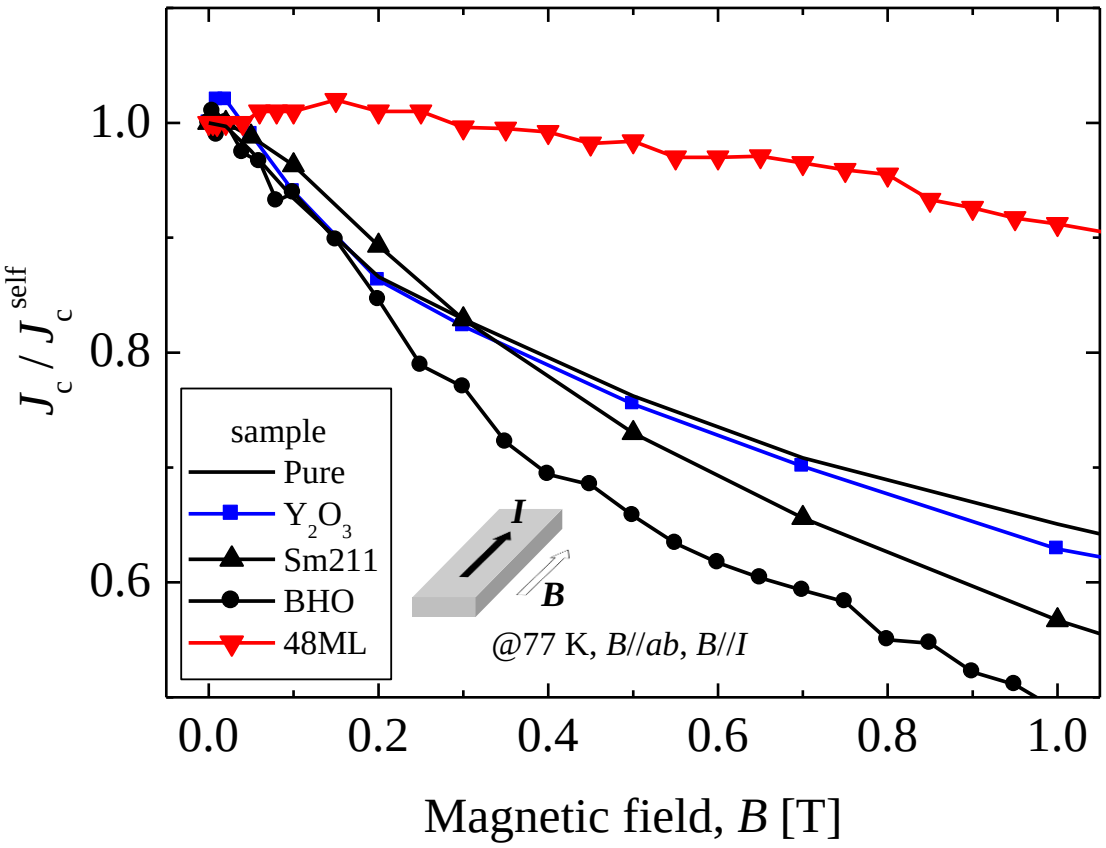

Figure2(b)

Magnified J_c-B curves normalized by J_c^{self}s in low-field region of each Sm123 film at 77 K in the LMF state.

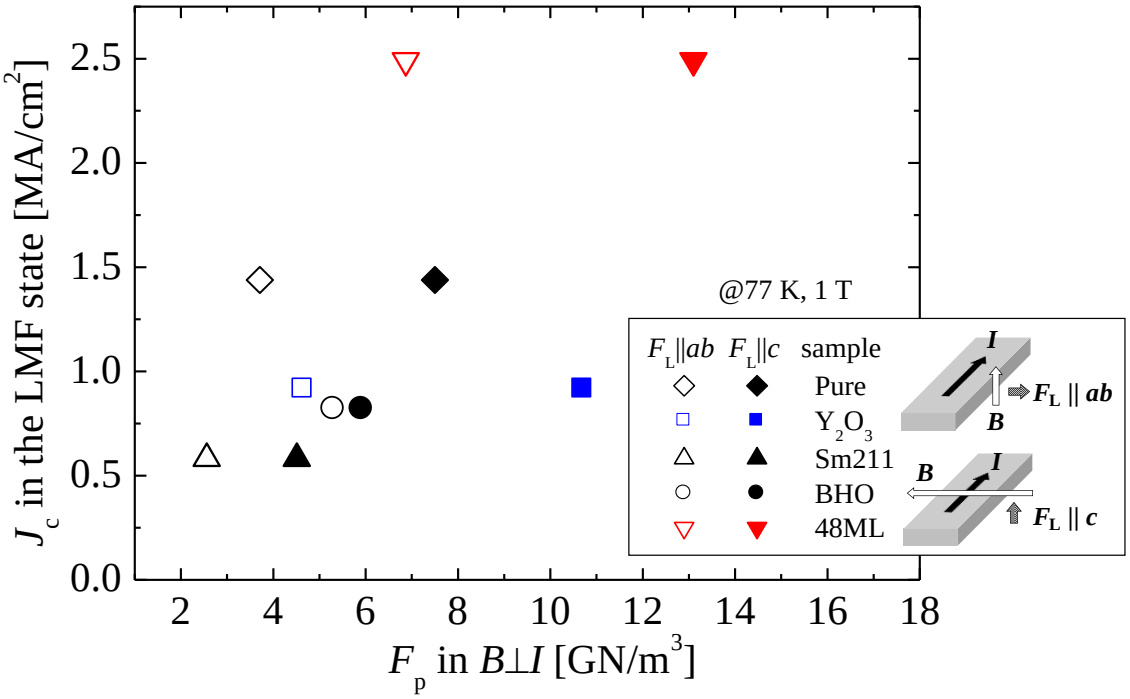

Figure 3

J_c in the LMF state as functions of F_ps in transverse field at 77 K in 1 T.

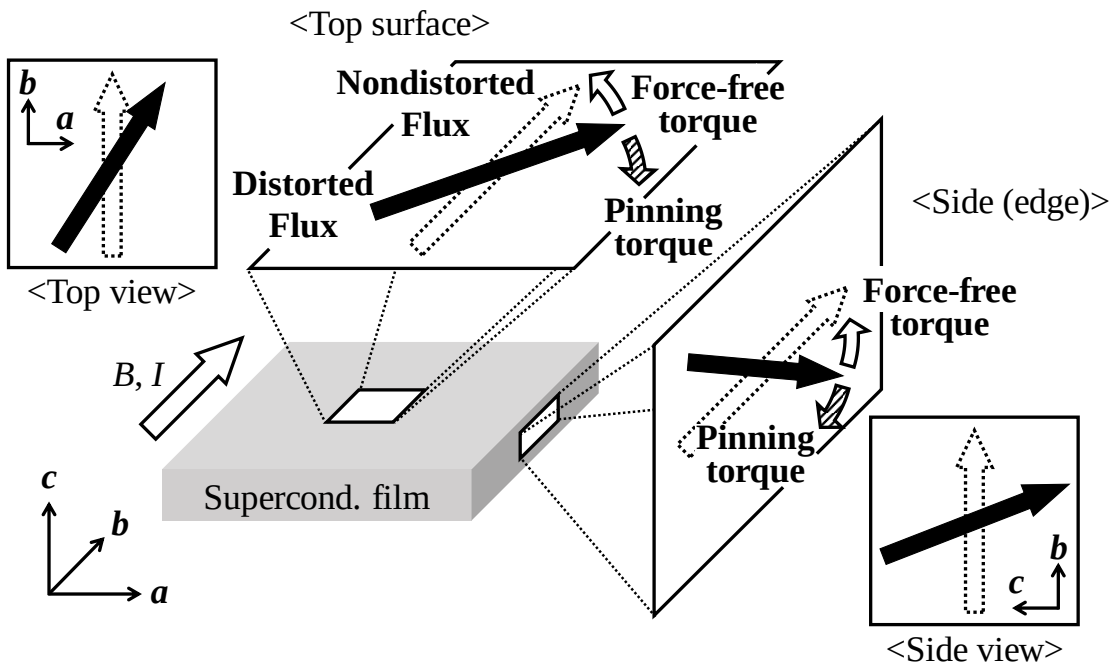

Figure 4

Schematic drawing of the flux motion and its pinning around the top surface and the side of the superconducting film in the LMF state:the distortion of flux lines in the side edge is larger than that in the top surface, because of a difference of the self-field magnitude caused by the film shape.